Journal of Alloys and Compounds 509 (2011) 5061–5063

Contents lists available at ScienceDirect

Journal of Alloys and Compounds

journal homepage: www.elsevier.com/locate/jallcom

High quality $TbMnO_3$ films deposited on $YAlO_3$

Artur Glavic[a,*], Jörg Voigt[b], Jörg Persson[a], Yixi Su[b], Jürgen Schubert[c], Joost de Groot[a], Willi Zande[c], Thomas Brückel[a,b]

[a] Institut für Festkörperforschung, Forschungszentrum Jülich, D-52425 Jülich, Germany
[b] Jülich Centre for Neutron Science, IFF, Forschungszentrum Jülich, Outstation at FRM II, Lichtenbergstrasse 1, D-85747 Garching, Germany
[c] Institute of Bio-and Nano-Systems (IBN1-IT), and JARA-Fundamentals of Future Information Technology, Research Centre Jülich, D-52425, Germany

ARTICLE INFO

Keywords:
Thin films
Multiferroics
Transition metal oxides

ABSTRACT

High quality thin films of $TbMnO_3$ were grown by pulsed laser deposition on orthorhombic$YAlO_3$ (1 0 0). The interface and surface roughness of a 55 nm thick film were probed by X-ray reflectometry and atomic force microscopy, yielding a roughness of 1 nm. X-ray diffraction revealed untwinned films and a small mosaic spread of 0.04° and 0.2° for out-of-plane and in-plane reflections, respectively. This high degree of epitaxy was also confirmed by Rutherford backscattering spectrometry. Using polarized neutron diffraction we could identify a magnetic structure with the propagation vector (0 0.27 0), identical to the bulk magnetic structure of $TbMnO_3$.

1. Introduction

"The revival of the magneto-electric effect" [1] was triggered strongly by the observation of multiferroic behavior in a variety of manganites containing small rare earth cations [2–4]. In these compounds a strong coupling exists between the ferroelectric polarization and the (anti)ferromagnetic order of their spin system [5]. From a theoretical point of view these compounds contradict the usual explanation for ferroelectricity and magnetic order in transition metal systems. The former usually requires d^0-ness, i.e. empty d orbitals, while the latter can only appear when partly filled 3d orbitals are present. From an application's point of view the control of the electrical degrees of freedom via magnetic fields and vice versa offers fascinating new perspectives, e.g. devices where a magnetic field changes the optical properties [6]. When it comes to devices thin films of multiferroic compounds are required. Furthermore, the mechanisms leading to multiferroic behavior may be altered by epitaxial strain or the increased importance of interfaces and finite size.

In $TbMnO_3$, the multiferroic properties have been attributed to its spiral spin structure occurring at low temperatures [7,8]. Thin films enable us to study the influence of finite size effects and crystallographic strain on the magnetic order of this compound. Mastering the growth of these films is a prerequisite to possible applications in multiferroic tunnel junctions. TbMnO3 thin films have already been grown on e.g. $SrTiO_3$ and $LaAlO_3$ substrates [9]. These films exhibit 90° twinning. $YAlO_3$ (1 0 0) [orthorhombic representation with *Pbnm* space group setting] was chosen as a substrate because of three major advantages. First there is only one growth direction for $TbMnO_3$ on the substrate, since it has in-plane lattice parameters of 5.31 Å and 7.35 Å close to $TbMnO_3$ a and c lattice constants (5.30 Å and 7.386 Å [10]), preventing twinning. Secondly, the out-of-plane lattice constant of $TbMnO_3$ and $YAlO_3$ are 5.81 Å [10] and 5.18 Å respectively, which allows the separation of the strong substrate signal and the weak film signal in diffraction techniques. Finally the propagation vector of the $TbMnO_3$ spin-spiral, as it is known from bulk [7,11–13], also lies in out-of-plane direction so that finite size effects can be expected for decreasing thickness in films or superlattices.

2. Sample preparation

The $TbMnO_3$ targets for pulsed laser deposition were produced by solid state synthesis from Tb4O7 and MnO2 powder. The primary materials were calcined for 6 h at 1100 °C then compressed 10 min under 0.13 GPa and subsequently sintered for 6 h at 1300 °C.The films were grown on the $YAlO_3$ substrates by pulsed laser deposition (PLD) under a constant oxygen flow with an energy density of 5 J/cm^2@10 Hz and parameters as shown in Table 1. Two types of films with 200 nm and 55 nm thickness were prepared with the setup described in [14].

3. Experimental results

3.1. X-ray diffraction

For the characterization of the crystalline quality an X-ray 4-circle diffractometer with Cu Kα radiation was used. Several

* Corresponding author.
E-mail address: artur.glavic@googlemail.com (A. Glavic).

0925-8388/$ – see front matter © 2011 Elsevier B.V. All rights reserved.
doi:10.1016/j.jallcom.2011.03.015

Table 1
Parameters of different PLD samples and their measured characteristics ordered by temperature. Values marked with minus could not be measured because of too low intensities. Bold text marks the samples used for the illustrated data. High resolution setup was used to measure rocking curves of out-of-plane reflections.

PLD parameters			Film thickness		FWHM of reflections in° (intensity c/s)		
Pulses	Temperature	O_2 pressure	X-ray	RBS	$(0\,2\,0)_{Refl.}$	$(0\,2\,l)_{4\text{–cric}}$	$(2\,2\,0)_{4\text{–cric}}$
1000	770 °C	5×10^{-3} mbar	54.9(5) nm		0.09 (4×10^2)		0.40 (4×10^2)
1000	740 °C	5×10^{-3} mbar	55(1) nm		0.05 (3×10^3)	0.35(1.0–10^3)	0.30 (8×10^2)
1000	710 °C	5×10^{-3} mbar	55.9(2) nm		0.04 (5×10^3)		0.40 (8×10^2)
3600	695 °C	5×10^{-3} mbar	–	200(10) nm	0.05 (3×10^4)		0.27 (3×10^3)
3600	695 °C	8×10^{-3} mbar			0.15(1×10^1)	-	–
1000	680 °C	5×10^{-3} mbar	55.0(5) nm		0.04 (6×10^3)	0.17(1.2×10^3)	0.14(2×10^3)
1000	670 °C	5×10^{-3} mbar	54.9(2) nm	55(5) nm	0.04 (5×10^3)	0.20 (1.5×10^3)	0.35 (6×10^2)
1000	645 °C	5×10^{-3} mbar	54.0(5) nm		0.03 (9×10^3)	0.16(0.7×10^3)	0.40 (6×10^2)

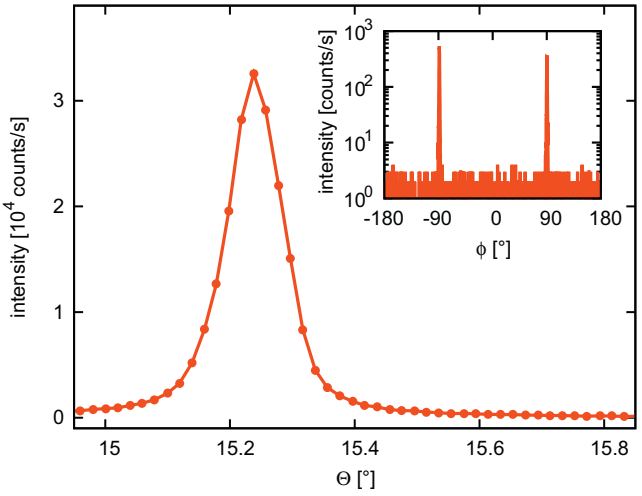

Fig. 1. Rocking curve of (0 2 0) reflection from 200 nm $TbMnO_3$, FWHM 0.1° (resolution limited). Inset: Phi scan of the (0 6 2) reflection (logarithmic scale) with the Phi axis aligned parallel to the (0 2 0) direction.

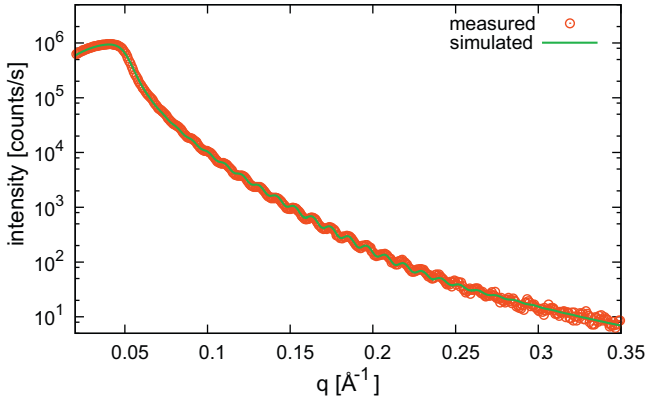

Fig. 2. X-ray reflectometry on 55.0(5) nm $TbMnO_3$ film on $YAlO_3$. Layer thickness 55 nm, rms roughness 0.8(1) nm and substrate rms roughness 0.3(1) nm were obtained by the fit. (For interpretation of the references to color in this figure legend, the reader is referred to the web version of the article.)

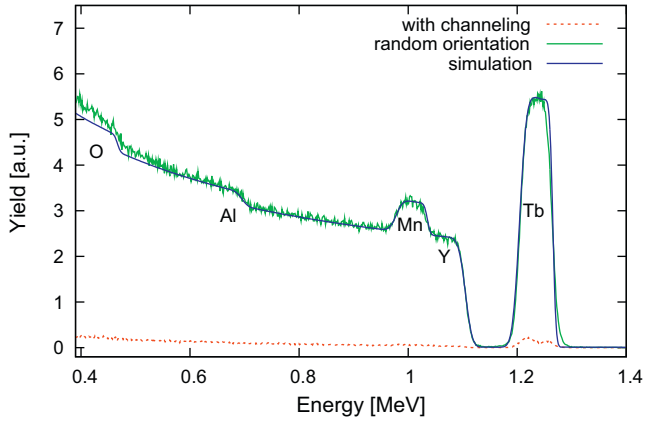

Fig. 3. RBS from $TbMnO_3$ film on $YAlO_3$ random oriented (light green) and with channeling (dashed red). The fit (dark blue) to the random curve leads to a thickness of 55(5) nm. (For interpretation of the references to color in this figure legend, the reader is referred to the web version of the article.)

(partly) in-plane and out-of-plane reflections from the substrate and the film, which were separated due to their different out-of-plane lattice spacings, were measured. The mosaic widths of the 200 nm and the 55 nm samples were comparable with approximately 0.04° out-of-plane and 0.15°–0.35° for in-plane reflections. The absence of twinning was confirmed by a 360° phi scan[1] of an in-plane reflection (0 6 2) showing only reflections separated by 180° (inset Fig. 1).

3.2. X-ray reflectometry

The film thickness and roughness over the whole sample was determined with a Bruker D8 X-ray reflectometer providing Cu Kα radiation. The parameters in Table 1 were obtained by fitting the data as exemplified in Fig. 2. The samples created with 1000 pulses were of 55.0(5) nm film thickness with an rms roughness of 0.8(1) nm and thickness variations[2] of approximately 1.0(3) nm over the 1 cm × 1 cm sample. This was confirmed by atomic force micrographs where the height standard deviation is about 1 nm over 3.5 μm × 3.5 μm. For a better resolution the out-of-planemosaic widths in Table 1 were also measured with the reflectometer.

3.3. Rutherford backscattering spectrometry

Additionally the samples were investigated by Rutherford Backscattering Spectrometry (RBS) using 1.4 MeV He^+ ions. Energy losses in the film can be simulated to obtain information about the structure. The film thickness obtained by reflectometry and RBS both match within the experimental limits (shown in Fig. 3). By channeling[3] an intensity drop to 2% was measured. This also con-

[1] In advance the sample alignment was checked with the (0 6 2), (0 6 − 2), (2 2 0) and (−2 2 0) reflections to be sure to probe the correct plane with the phi scan.

[2] Thickness variations on larger lateral length scales have been taken into account by summing up the intensities of different simulations.

[3] Uniform alignment of the incidence beam parallel to a high symmetry axis of the crystal.

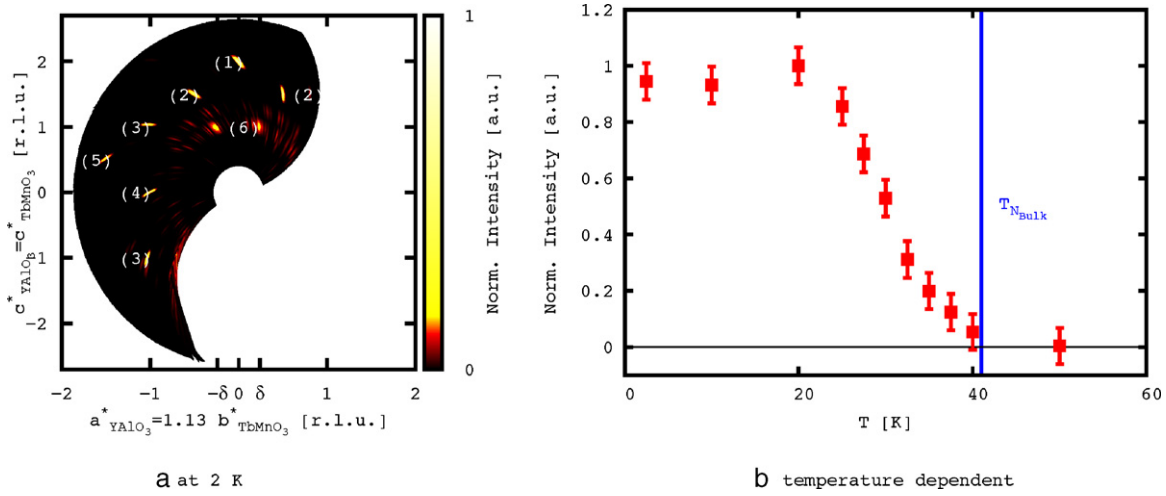

Fig. 4. Spin-flip channel of polarized neutron diffraction from a 200 nm $TbMnO_3$ film. The scattering plane was the $TbMnO_3$ bc-plane ($YAlO_3$ ac-plane) with the polarization vector in *a* direction at 2 K (left). The numbered reflections are: (1) and (3): $YAlO_3$ (0 0 2) and (±1 0 1) reflections visible due to a finite flipping ratio of ≈30; (2), (4) and (5): $YAlO_3$ (±1 0 3), (2 0 0) and (3 0 ±1) reflections from λ/2 and (6): $TbMnO_3$ film (0 δ 1) magnetic reflection respectively. The magnetic reflection (0 δ 1) was also measured temperature dependent (right). The integrated intensities of the magnetic peak show a transition temperature comparable to bulk.

firmed the good crystalline quality deduced from the diffraction data. As the reflectometer resolution limited the thickness determination to films <100 nm thickness, RBS was used for films of larger thickness.

3.4. Polarized neutron diffraction

The magnetic structure of the thin films was investigated by polarized neutron diffraction at the DNS instrument of the FRM II reactor in Garching. Since neutron diffraction studies of thin films are difficult due to the fact that the signal of the substrate dominates the diffraction pattern, we reduced this intensive "background" choosing the scattering geometry in combination with longitudinal polarization analysis. The sample was mounted with the [1 0 0] direction of $TbMnO_3$ vertically, so reflections of type (0 *k l*) were accessible in the horizontal plane. Thus different types of magnetic reflections observed in the bulk [7,13] could be reached. In theory, for perfect neutron polarization parallel to [1 0 0], the [0 1 0] and [0 0 1] components of the magnetic moment contribute to spin-flip scattering only, while the [1 0 0] component and the nuclear scattering are only observed in the non spin-flip channel [15]. In practice we achieved a decrease of a factor of 30 in the substrate background for the scattering channel that probed the bulk chiral plane.

Fig. 4(a) shows a color plot of the diffracted intensity in the spin-flip channel measured at 2 K. The map was recorded by rotation of the sample through a range of 200° with a step size of 1°. The data are corrected for detector efficiency, using a Vanadium standard, and background. The substrate reflections are still identifiable as well as the corresponding λ/2 reflections (as the substrate is 0.5 mm thick, even a good flipping-ratio of about 30 does not suppress these reflections entirely). The reflections labeled (6) appear exactly at the positions of the magnetic Mn ordering in bulk (0 0.27 1) [7,11]. The temperature dependence of the magnetic reflection (0 δ 1) is illustrated in Fig. 4(b) with an integrated intensity that vanishes at about 40 K which also matches the bulk values. Here we rotated the sample only through a small angular range to determine the integrated intensity of the reflection. The thin film apparently developed a similar magnetic structure as found in the bulk.

4. Conclusion

In summary, we were able to grow highly epitaxial thin films of $TbMnO_3$ without any twinning. As shown in Table 1 the best crystallinity is obtained at a substrate temperature of 680 °C and an oxygen pressure of 5×10^{-3} mbar. X-ray diffraction confirmed the absence of twinning. Long range magnetic ordering in the films, similar to the bulk magnetic structure, was evidenced by polarized neutron diffraction. In contrast to $TbMnO_3$ films grown on $SrTiO_3$, which exhibit ferromagnetic ordering (eliminating the ferroelectric property), the films grown on $YAlO_3$ remain antiferromagnetic. As has already been proposed by Kirby et al. [16], the ferromagnetism is likely to be induced by the compressive strain of the substrate (which changes the Mn–O–Mn angle in $TbMnO_3$), which is not present in the system investigated here. This fact demonstrates the rich physics that can be found in $TbMnO_3$ by additionally investigating thin films and interfaces to other materials.

References

[1] M. Fiebig, Journal of Physics D Applied Physics 38 (8) (2005) R123–R152.
[2] T. Kimura, T. Goto, H. Shintani, K. Ishizaka, T. Arima, Y. Tokura, Nature 426 (6962) (2003) 55–58, doi:10.1038/nature02018.
[3] T. Kimura, G. Lawes, T. Goto, Y. Tokura, A. Ramirez, Physical Review B 71 (22) (2005) 224425, doi:10.1103/PhysRevB.71.224425.
[4] N. Hur, S. Park, P.A. Sharma, J.S. Ahn, S. Guha, S.W. Cheong, Nature 429 (2004) 392–395.
[5] W. Eerenstein, N.D. Mathur, J.F. Scott, Nature 442 (7104) (2006) 759–765.
[6] M. Bibes, A. Barthelemy, Nature Materials 7 (6) (2008) 425–426.
[7] M. Kenzelmann, A.B. Harris, S. Jonas, C. Broholm, J. Schefer, S.B. Kim, C.L. Zhang, S.W. Cheong, O.P. Vajk, J.W. Lynn, Physical Review Letters 95 (8) (2005) 087206.
[8] N. Nagaosa, Journal of Physics: Condensed Matter 20 (43) (2008) 434207.
[9] Y. Cui, C. Wang, B. Cao, Solid State Communication 133 (10) (2005) 641–645, doi:10.1016/j.ssc.2005.01.002.
[10] J. Blasco, C. Ritter, J. Garcia, J. de Teresa, J. Perez-Cacho, M. Ibarra, Physical Review B 62 (9) (2000) 5609–5618.
[11] J. Voigt, J. Persson, J.W. Kim, G. Bihlmayer, T. Brückel, Physical Review B 76 (10) (2007) 104431.
[12] S. Quezel, F. Tcheou, J. Rossatmignod, G. Quezel, E. Roudaut, Physica B & C 86 (1977) 916–918.
[13] R. Kajimoto, H. Yoshizawa, H. Shintani, T. Kimura, Y. Tokura, Physical Review B 70 (1) (2004) 012401.
[14] C. Buchal, L. Beckers, A. Eckau, J. Schubert, W. Zander, Materials Science Engineering B-Solid State Matererials Advance Technology 56 (2–3) (1998) 234–238.
[15] R.M. Moon, T. Riste, W.C. Koehler, Physical Review 181 (2) (1969) 920–931.
[16] B.J. Kirby, D. Kan, A. Luykx, M. Murakami, D. Kundaliya, I. Takeuchi, Journal of Applied Physics 105 (7) (2009) 07D917.